arXiv:1511.07264v1 [cond-mat.mes-hall] 23 Nov 2015

Nonlocal spin torques in Rashba quantum wires with steep magnetic textures

Martin Stier and Michael Thorwart
I. Institut für Theoretische Physik, Universität Hamburg, Jungiusstraße 9, 20355 Hamburg, Germany

We provide a general procedure to calculate the current-induced spin-transfer torque which acts on a general steep magnetic texture due to the exchange interaction with an applied spin-polarized current. As an example, we consider a one-dimensional ferromagnetic quantum wire and also include a Rashba spin-orbit interaction. The spin-transfer torque becomes generally spatially non-local. Likewise, the Rashba spin-orbit interaction induces a spatially nonlocal field-like nonequilibrium spin-transfer torque. We also find a spatially varying nonadiabaticity parameter and markedly different domain wall dynamics for very steep textures as compared to wide domain walls.

PACS numbers: 75.78.Fg, 75.70.Tj, 75.25.-b

The exchange interaction of a spin-polarized electron current with localized magnetic moments in a ferromagnetic wire typically induces a spin transfer torque (STT). A pronounced consequence is the coordinated switching of the localized magnetic moments of a ferromagnetic domain wall (DW) in the wire generating a net DW motion [1–3]. Other magnetic textures also rose to recent prominence, such as magnetic vortices and skyrmions [4–6], or one-dimensional spin chains[7]. There, the magnetization changes on much shorter length scales as compared to the conventional broad mesoscopic Bloch domain walls. In addition, these textures are in general strongly affected by symmetry breaking interactions, such as the spin-orbit [8] or the Dzyaloshinskii-Moriya interaction [9, 10].

Clearly, in small structures, the backaction of the local magnetic moments on the polarized itinerant electron spins can become relevant. In particular, they themselves experience a back-acting STT as well. For wide magnetic textures, the impact of backaction is generally small since the itinerant spins relax much faster than they have time to interact with the local moments. Hence, for wide textures, it is reasonable to assume a stationary spin polarized current which generates the (non-)adiabatic STT [11]. This assumption, however, becomes increasingly invalid in more narrow or steep magnetic textures. In this context, questions have been raised why the nonadiabaticity parameter β is much larger in small vortex structures [12, 13] than compared to spin-waves in extended structures [14]. This effect has been traced back to a non-standard description of the STT [15].

For a unified description of the STT for arbitrary magnetic textures, several approaches have been developed [15–22]. Nevertheless, a complete picture is still missing. Spin relaxation has either been neglected [16, 17] or included [18–20], quantum corrections are considered[23] or a semiclassical approach on the basis of spin diffusion has been formulated [15, 24]. Spin-orbit interaction has been considered for broad textures [21, 22] only.

In this work, we provide a general and conceptually simple scheme to calculate the STT for arbitrary magnetic textures. To show the flexibility of the approach, we also include the Rashba spin-orbit interaction in the itinerant electrons, whose contribution to the STT in steep magnetic structures is of high interest [25, 26]. The STT and the resulting nonadiabatic Rashba field-like STT are shown to become non-local in space for steep textures. The known results for broad Bloch DWs [27–29] are recovered as a limiting case. We calculate DW velocities for a broad range of widths of a Bloch DW and find a non-local nonadiabaticity parameter for steep textures. Interestingly, the overall direction of the DW movement can be determined by the DW width.

We consider a one-dimensional (1D) ferromagnetic quantum wire with a magnetic texture formed by localized magnetic moments $M_s\mathbf{n}(x,t)$ with a saturation magnetization M_s and unit vectors $\mathbf{n}(x,t)$. Their dynamics follows from the Landau-Lifshitz-Gilbert (LLG) equation

$$\partial_t \mathbf{n} = -\gamma_0 \mathbf{n} \times \mathbf{H}_{\text{eff}} + \alpha \mathbf{n} \times \partial_t \mathbf{n} + \mathbf{T} \,, \tag{1}$$

with the effective magnetic field $\mathbf{H}_{\text{eff}}$, the gyro-magnetic ratio γ_0, and the Gilbert damping constant α. $\mathbf{T}$ denotes the spin torque which is induced by the exchange interaction of the localized moments with the polarized spins of the current carrying electrons. The latter and the interaction are described by the Hamiltonian

$$H = H_{\text{kin}} + H_{\text{Rashba}} + H_{\text{sd}} + H_{\text{relax}} \,. \tag{2}$$

It contains the kinetic energy, the Rashba spin-orbit interaction, the *sd* interaction with the magnetic moments and the relaxation of the electron spins. It is convenient to use the low-energy description of this Hamiltonian, as it is accurate for 1D quantum wires [30] and yields a simple derivation of the STT [27, 28]. Then, all relevant electron operators $c_\sigma, c_\sigma^\dagger$ with spin index σ can be included in spin-like operators $\hat{\mathbf{J}}_r = \frac{1}{2} : c_{r\sigma}^\dagger \boldsymbol{\sigma}_{\sigma\sigma'} c_{r\sigma'} :$. The index $r = R/L = +/-$ refers to right or left moving electrons in the wire. The Rashba Hamiltonian assumes the simple form $H_{\text{Rashba}} = \Delta_{\text{R}} \sum_r p \int dx \; \hat{\mathbf{J}}_r \cdot \mathbf{e}_y$, with the Rashba splitting $\Delta_{\text{R}} = 2\tilde{\alpha}_{\text{R}} k_F$[29]. All terms of Eq. (2) can be expressed in terms of $\hat{\mathbf{J}}_r$, for which the Heisenberg equations of motion $\partial_t \hat{\mathbf{J}}_r = -\frac{i}{\hbar}\left[\hat{\mathbf{J}}_r, H\right]_-$ can readily be evaluated [27–29]. We find for the expectation

value $\mathbf{J}_r = \langle \hat{\mathbf{J}}_r \rangle$

$$\partial_{(r)} \mathbf{J}_r = -\frac{\Delta_{\rm sd}}{\hbar}[\mathbf{J}_r \times \mathbf{m}_r + \beta(\mathbf{J}_r - \mathbf{J}_r^{\rm rel})] \,, \qquad (3)$$

with the derivative $\partial_{(r)} = \partial_t + vr\partial_x$, $\mathbf{m}_r = \mathbf{n} + r\alpha_{\rm R}\mathbf{e}_y$, the Fermi velocity v, the exchange interaction strength $\Delta_{\rm sd}$, the Rashba parameter $\alpha_{\rm R} = \Delta_{\rm R}/\Delta_{\rm sd}$, the nonadiabaticity parameter $\beta = \hbar/(\Delta_{\rm sd}\tau)$, relaxation time τ and the relaxed spin density $\mathbf{J}_r^{\rm rel}$. In fact, this is the continuity equation of the spin current[31–34] when we introduce the spin density $\mathbf{s} = \mathbf{J}_R + \mathbf{J}_L$ and the spin current density $\mathbf{J} = v(\mathbf{J}_R - \mathbf{J}_L)$ and sum over r.

To solve the equations of motion (3), we set up the ansatz

$$\mathbf{J}_r = a_r \overline{\mathbf{m}}_r + b_r \overline{\partial_{(r)}\mathbf{m}}_r + c_r \overline{\mathbf{m}}_r \times \overline{\partial_{(r)}\mathbf{m}}_r \,, \qquad (4)$$

with the unit vectors $\overline{\mathbf{m}}_r = \mathbf{m}_r/|\mathbf{m}_r|$ and $\overline{\partial_{(r)}\mathbf{m}}_r = \partial_{(r)}\overline{\mathbf{m}}_r/|\partial_{(r)}\overline{\mathbf{m}}_r|$. It is the central observation of this work to use space- and time-dependent coefficients $a_r(x,t), b_r(x,t), c_r(x,t)$. All three vectors in Eq. (4) form a complete orthonormal basis in spin space. With the prefactors determined below, the STT $\mathbf{T} = -\frac{\Delta_{\rm sd}}{\hbar}\mathbf{n}\times\mathbf{s} = -\frac{\Delta_{\rm sd}}{\hbar}\mathbf{n}\times\sum_r \mathbf{J}_r$ can be calculated. Straightforward algebra yields

$$\mathbf{T} = \sum_{\nu=x,t} \left[T_\nu^{\rm nonad}(b_r)\overline{\partial_\nu \mathbf{n}} + T_\nu^{\rm ad}(c_r)\mathbf{n}\times\overline{\partial_\nu\mathbf{n}}\right] - H_{\rm R}(a_r,b_r)\mathbf{n}\times\mathbf{e}_y \,. \qquad (5)$$

In particular, the ansatz yields the adiabatic STT $T_{x,t}^{\rm ad}$, the nonadiabatic STT $T_{x,t}^{\rm nonad}$, as well as the field-like Rashba term with the nonadiabatic Rashba field $H_{\rm R}$. By construction, the antidamping field $\mathbf{H}_{\rm R}^{\rm anti} = -\beta\mathbf{n}\times\mathbf{H}_{\rm R}$ is included, although it does not appear explicitly. It easily can be recovered by choosing a suitable overcomplete basis in the ansatz (4). Notice that we have defined the STT in terms of the normalized vectors of the derivative $\overline{\partial_x\mathbf{n}} = \partial_x\mathbf{n}/|\partial_x\mathbf{n}|$ to avoid a divergence of the prefactors. In general, also terms $\propto \partial_t\mathbf{n}, \mathbf{n}\times\partial_t\mathbf{n}$ appear. They act as additional damping terms in Eq. (1) and are conveniently absorbed in a rescaled Gilbert parameter.

The remaining step is to determine the coefficients a_r, b_r and c_r. For this, we insert the Ansatz Eq. (4) into Eq. (3) and order it according to linearly independent parts. This yields to an ordinary differential equation

$$\partial_{(r)}\begin{pmatrix} a_r \\ b_r \\ c_r \end{pmatrix} = A_r \begin{pmatrix} a_r \\ b_r \\ c_r \end{pmatrix} + \frac{\Delta_{\rm sd}\beta}{\hbar}\begin{pmatrix} a_r^{\rm rel} \\ b_r^{\rm rel} \\ c_r^{\rm rel} \end{pmatrix} , \qquad (6)$$

where $a_r^{\rm rel}$, $b_r^{\rm rel}$ and $c_r^{\rm rel}$ are the corresponding coefficients of the relaxed spin density $\mathbf{J}_r^{\rm rel}$. The coefficient matrix

$$A_r = \begin{pmatrix} -\Delta_{\rm sd}\beta/\hbar & |\partial_{(r)}\overline{\mathbf{m}}_r| & 0 \\ -|\partial_{(r)}\overline{\mathbf{m}}_r| & -\Delta_{\rm sd}\beta/\hbar & -\Delta_{\rm sd}|\mathbf{m}_r|/\hbar - g \\ 0 & \Delta_{\rm sd}|\mathbf{m}_r|/\hbar + g & -\Delta_{\rm sd}\beta/\hbar \end{pmatrix} \qquad (7)$$

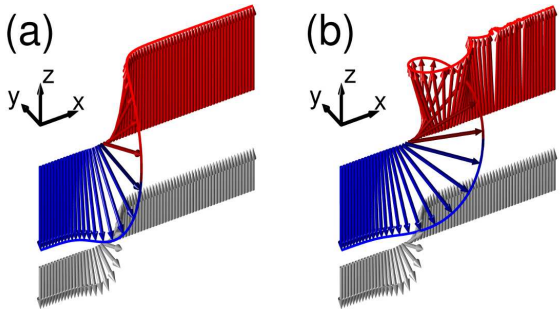

FIG. 1. (Color online) Sketch of the configurations of the localized DW spins (gray arrows) and the itinerant spins flowing from negative to positive x-values, for a broad (a) and a steep (b) domain wall (distances are normalized to the DW width). Red (blue) arrows show the direction of the z-component of the itinerant spins in positive (negative) direction. The lines are guides for the eyes. While for broad DWs ($\lambda \gg x_{\rm osc}^{\infty}$), the itinerant spins follow the DW magnetization adiabatically, this is not possible for steep DWs ($\lambda \leq x_{\rm osc}^{\infty}$).

is space- and time-dependent due to $|\partial_{(r)}\overline{\mathbf{m}}_r|(x,t)$ and $g = [\partial_{(r)}\overline{\mathbf{m}}_r \cdot (\overline{\mathbf{m}}_r \times \partial_{(r)}^2\overline{\mathbf{m}}_r)]/(\partial_{(r)}\overline{\mathbf{m}}_r)^2$. Hence, a general analytical solution of Eq. (6) cannot be found. Even though these equations are derived within a 1D model, they readily can be used for higher dimensional magnetic textures, if the electronic motion perpendicular to the current is less important.

In the following, we solve Eq. (6) numerically for the example of a Bloch DW. Other textures can be treated in the similar way. As both Eqs. (6) and (1) depend on $\mathbf{n}$, it is necessary to solve them self-consistently for each time step until convergence is achieved. This is still demanding and we can use physical arguments to further simplify the equation. First, we may assume that all coefficients depend only on the distance to the DW center $x_{\rm DW}(t)$, since we do not consider explicit time-dependent modifications of the shape of the initially prepared domain wall [27]. Hence, $a_r(x,t) = a_r[\Delta x = x - x_{\rm DW}(t)]$. Then, it follows that $\partial_{(r)}a_r(\Delta x) = [pv - \partial_t x_{\rm DW}(t)]\partial_{\Delta x}a_r(\Delta x)$. As the DW velocity $\partial_t x_{\rm DW}(t)$ is generally much smaller than the Fermi velocity v, we can neglect the terms involving $\partial_t x_{\rm DW}(t)$. Effectively, every time derivative in Eq. (6) is neglected, and thereby also the damping parts in Eq. (5). We do not simplify the LLG equation (1) by this assumption, so that a precessional motion of the DW is still possible.

Before we discuss the numerical results, it is instructive to analyze the generic qualitative behavior which can be extracted from Eq. (6). The eigenvalues of the matrix in Eq. (7) are of the form $\xi_1 = -\beta\Delta_{\rm sd}/(\hbar v)$ and $\xi_\pm = [-\beta\Delta_{\rm sd} \pm i\sqrt{(\Delta_{\rm sd}|\mathbf{m}_r| + g)^2 + (\hbar v\partial_x|\mathbf{m}_r|)^2}]/(\hbar v)$. For constant coefficients, the solutions of Eq. (6) would be combinations of exponentials $\propto \exp(\xi_i x)$. Thus, the real part $\mathrm{Re}\,\xi_i$ determines a damped, and the imaginary part $\mathrm{Im}\xi_i$ an oscillating behavior. As the real part is

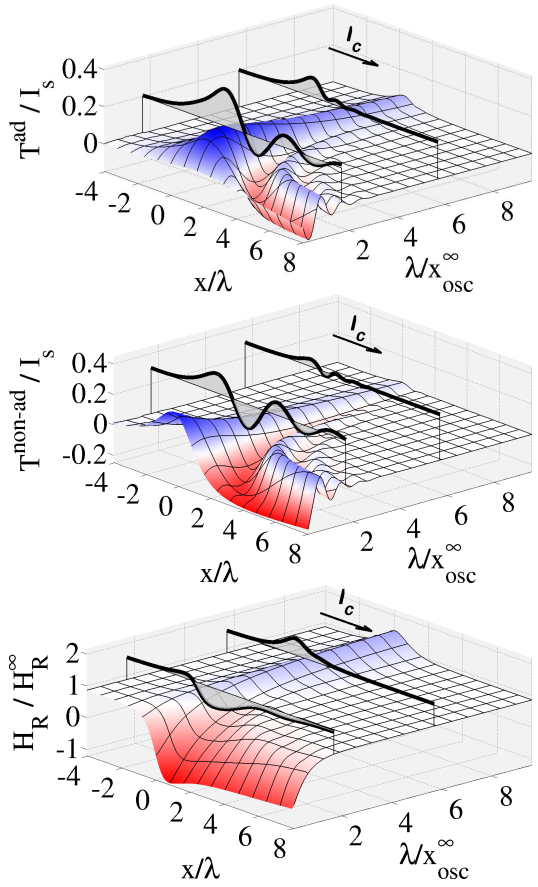

FIG. 2. (Color online) Spatial dependence of the three components to the STT: the adiabatic STT (top), the nonadiabatic STT (middle), and, the Rashba field-like term (bottom) for varying DW widths λ. Blue (red) colors indicate positive (negative) deviation from their relaxed values. Two cases for $\lambda/x_{\rm osc}^\infty = 1.7, 5.7$ are highlighted (shifted thick black curves). The parameters are $\alpha_{\rm R} = 0.4$, $\beta = 0.2$.

the same for all ξ_i, we find a unique damping length $x_{\rm damp} = \hbar v/(\beta\Delta_{\rm sd})$. The oscillation length $2\pi x_{\rm osc}$ can only be estimated. Far away from the DW center, when $|\partial_x \overline{\mathbf{m}}_r| \propto |\partial_x \mathbf{n}| = 0$, it is determined by the inverse *sd* coupling strength such that $x_{\rm osc} \approx x_{\rm osc}^\infty \equiv \hbar v/\Delta_{\rm sd}$. Close to the DW center, $x_{\rm osc}$ is modified by the term $|\partial_x \overline{\mathbf{m}}_r| \propto 1/\lambda$, where λ is the DW width. Thus, in particular for steep DWs, the oscillation period is reduced.

The qualitative observations are supported by explicit numerical calculations. We consider a Bloch-z DW with boundary conditions $n_z(x \to \pm\infty) = \pm 1$. The DW is formed by the effective field $\mathbf{H}_{\rm eff} = (2A_{\rm ex}/M_s)\partial_x^2\mathbf{n} + K_\parallel n_\parallel \mathbf{e}_\parallel - K_\perp n_\perp \mathbf{e}_\perp$, with an easy (hard) axis along $\mathbf{e}_{\parallel(\perp)}$. Further, we choose the physical parameters of Pt/Co/AlO$_x$ and set $A_{\rm ex} = 10^{-11}$J/m and $M_s = 1090$kA/m. In addition, we fix $\alpha = 0.1$ and set $\Delta_{\rm sd} = 0.25$eV, $v_F = 10^6$m/s and the current's polarization $P = 1$. The Rashba interaction is chosen around $\tilde{\alpha_{\rm R}} = 10^{-10}$eVm corresponding to $\Delta_{\rm R} = 0.1$eV and $\alpha_{\rm R} = \Delta_{\rm R}/\Delta_{\rm sd} = 0.4$. We vary the DW width $\lambda = \sqrt{J/K_\parallel}$, with $J = 2A_{\rm ex}/M_s$, by setting $J = \lambda J^{(0)}$ and $K_\parallel = K_\parallel^{(0)}/\lambda$ for a fixed ratio $\sqrt{J^{(0)}/K_\parallel^{(0)}} = 1$. The perpendicular anisotropy is set to $K_\perp = 0.3K_\parallel$. We inject polarized electrons from the right in their relaxed state. Thus, $\mathbf{J}_R(x \to -\infty) = \mathbf{J}_R^{\rm rel}$, with $\mathbf{J}_R^{\rm rel} = (I_s/v)\mathbf{n}$ with the saturation spin current $I_s \equiv PI_c/(2eM_s)$. Moreover, we use the oscillation period $x_{\rm osc}^\infty = \hbar v/\Delta_{\rm sd} = 2.6$ nm as a length scale. This uniquely determines the initial values of Eq. (6).

Two typical situations emerge and are illustrated in Fig. 1. For broad DWs, the itinerant spins follow the DW adiabatically. In contrast, for steep DWs, the spins experience a mismatch of $\mathbf{n}$ and $\mathbf{J}_R$ particularly at and beyond the DW center. This induces a significant backaction on the STT. In Fig. 2, the three contributions to $\mathbf{T}$ are shown for varying DW widths. For broad DWs ($\lambda \gg x_{\rm osc}^\infty$), the conventional contributions $T^{\rm ad} = I_s|\partial_x\mathbf{n}|$, $T^{\rm nonad} = -\beta I_s|\partial_x\mathbf{n}|$ and $H_{\rm R}^\infty = \Delta_{\rm sd}\alpha_{\rm R} I_s/(v\hbar\gamma_0)$ are recovered (cf. Appendix). In fact, Eq. (6) contains these solutions for $\lambda \to \infty$. Differences occur for the Rashba field-like torque due to corrections in first order in the derivative of the magnetization [28, 29]. In contrast, for steep DWs ($\lambda < x_{\rm osc}^\infty$), every STT component is altered. In particular, both the adiabatic and the nonadiabatic STT show spatial oscillations which are damped after crossing the DW with the damping length $x_{\rm damp} = \hbar v/(\beta\Delta_{\rm sd}) = \beta^{-1}x_{\rm osc}^\infty$. For sharp DWs ($\lambda \ll x_{\rm osc}^\infty$), the adiabatic STT is suppressed while the nonadiabatic STT is strongly increased. This behavior is even more pronounced when we exclude relaxation ($\beta = 0$). Then, the oscillations remain undamped beyond the DW (cf. Appendix). Besides the (non)adiabatic STT, the Rashba field-like torque is also enhanced and may even change its sign at the DW center. As we solved Eq. (6) exactly no divergent terms appear for $\mathbf{H}_{\rm R}$ which could be the case in approximate calculations[29].

An interesting quantity for technological applications is the velocity of the DW center for a given applied current density I_c. We show the results for the combinations of $\beta = 0$, $\beta = 0.2$, $\alpha_{\rm R} = 0$ and $\alpha_{\rm R} = 0.4$ in Fig. 3. For broad DWs in absence of the Rashba coupling ($\lambda \gg x_{\rm osc}^\infty$ and $\alpha_{\rm R} = 0$), we recover the well-known results. Without relaxation, $\beta = 0$, and for small currents, there is no DW movement. A finite velocity $\langle v_{DW}\rangle$ arises when the current density exceeds a critical value. For a finite $\beta = 0.2 = 2\alpha$, the Walker breakdown is observed, i.e., a strong increase of the velocity for small current and a decrease beyond a critical I_c.

However, the picture changes significantly for steep DWs. Here, even for $\beta = 0$, a finite DW velocity arises for $0 < \lambda < x_{\rm osc}^\infty$. It actually resembles the Walker breakdown for $\beta > \alpha$ in the case of broad DWs. For $\lambda \to 0$, the DW velocity decreases again.

A finite Rashba field-like STT for $\alpha_{\rm R} = 0.4$ mainly af-

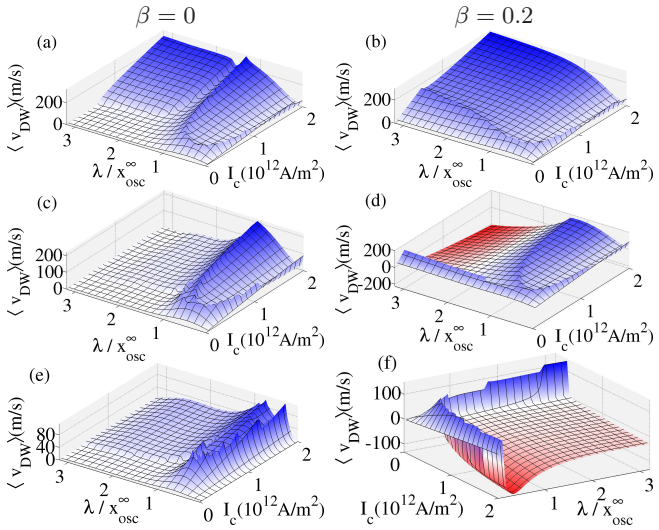

FIG. 3. (Color online) DW velocity vs DW width λ and applied current density I_c for the cases without relaxation ($\beta = 0$) in (a,c,e), for a finite relaxation ($\beta = 0.2$) in (b,d,f) for either vanishing Rashba coupling ($\alpha_{\rm R} = 0$) (a,b), finite $\alpha_{\rm R} = 0.4$ (c,d), or, for a width dependent $\alpha_{\rm R} = 0.4\frac{2}{\lambda/x^{\infty}_{\rm osc}}$ (e,f). Blue (red) colors emphasize a positive (negative) velocity.

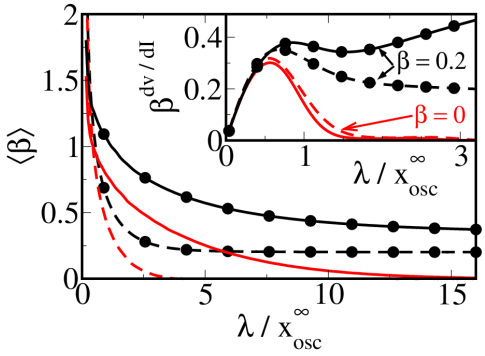

FIG. 4. (Color online) Averaged nonadiabaticity parameter $\langle\beta\rangle$ vs DW width for $\beta = 0$ (red, no symbols) and $\beta = 0.2$ (black, circles). Solid lines correspond to $\alpha_{\rm R} = 0.4$ while dashed lines refer to $\alpha_{\rm R} = 0$. The inset shows β^{dv/dI_c} obtained from the derivative dv/dI_c at small $I_c \to 0$. The values in the inset are normalized such that $\beta^{dv/dI_c}(\lambda \to \infty, \alpha_{\rm R} = 0) = \beta$.

fects broad DWs, since the nonadiabatic STT only can be dominant for narrow DWs. So far, we have assumed a constant Rashba coupling independent of λ. Thus, the Rashba field-like torque is comparable for all λ and every magnetic field, such as an externally applied global field, moves broader DWs faster [35]. To remove this trivial width dependence, we introduce a rescaled $\alpha_{\rm R} = 0.4\frac{2}{\lambda/x^{\infty}_{\rm osc}}$. Indeed, the DW velocity then becomes independent of λ for broad DWs. However, for small λ, a strong influence of $\mathbf{H}_{\rm R}$ on $\langle v_{DW}\rangle$ arises. In particular, for a finite β, even a substantial backward motion of the DW can be generated. The motion of the DW against the current flow is induced by the antidamping field [29, 36] $\mathbf{H}_{\rm R}^{\rm anti}$ which is implicitly included in the STT.

It is illuminating to discuss the case of small λ in terms of the nonadiabaticity parameter $\beta^* = T^{\rm nonad}/T^{\rm ad}$ [15]. For a nonlocal STT, β^* becomes x-dependent with singularities at the roots of $T^{\rm ad}$. Hence, an averaged nonadiabaticity parameter

$$\langle\beta\rangle = \frac{\int \beta^*(x)(\partial_x \mathbf{n})^2 dx}{\int (\partial_x \mathbf{n})^2 dx} \qquad (8)$$

has been introduced [15]. In Fig. 4, we show $\langle\beta\rangle$ for small current densities. For broad DWs and $\alpha_{\rm R} = 0$, the expected result $\langle\beta\rangle = \beta$ is recovered. In contrast, for steep DWs, $\lambda \lesssim x^{\infty}_{\rm osc}$, the nonadiabaticity strongly increases. This clearly shows that the standard description of the STT fails. What is more, for finite $\alpha_{\rm R}$, even for broad DWs, it holds that $\langle\beta\rangle \neq \beta$, because the (non)adiabatic STT also implicitly includes the antidamping field and the standard solutions for these STTs no longer hold.

An alternative characterization of the nonadiabaticity results from observing that, for a constant STT, the DW velocity increases with $\mathrm{d}\langle v_{DW}\rangle/\mathrm{d}I_c \propto \beta$ for small current densities [37]. Thus, we define $\beta^{\mathrm{dv/dI_c}}$ by the derivative of the DW velocity with respect to I_c and normalize it to the conventional β valid for large λ. The inset in Fig. 4 shows that also $\beta^{\mathrm{dv/dI_c}}$ becomes maximal around $\lambda \approx x^{\infty}_{\rm osc}$, but approaches zero for $\lambda \to 0$. This further underpins the non-trivial behavior for steep DWs which is not captured by the average $\langle\beta\rangle$.

Finally, our findings apply also to magnetic textures other than Bloch DWs. For example, the increase of the nonadiabaticity in steep textures is responsible for the differences between steep vortices and broad spin waves [13, 14], with an increased $\beta^{\rm vortex} \approx 5\beta^{\rm spin\text{-}waves}$.

In summary, we have introduced a general procedure to calculate the complete spin-transfer torque in arbitrary 1D magnetic textures. It applies to the entire range of steep to broad domain walls and also can include other symmetry breaking interactions. Here, we have discussed the Rashba spin-orbit interaction. For abrupt changes of the magnetic texture, the STT, the DW velocity and the nonadiabaticity are qualitatively modified including backward motion of steep DWs against the current. This shows that steep magnetic textures require a fully nonadiabatic description. An extension to two-dimensional structures such as vortices or skyrmions is straight-forward for the case of vanishing Rashba coupling, while current flow perpendicular to the direct current has to be considered for finite couplings.

We acknowledge support from the DFG SFB 668 (project B16).

Appendix

In this Appendix, we present the full explicit equations for the spin-transfer torque (STT) calculated from the differential equation (6). In addition, we solve this differential equation in the limiting case of infinitely wide domain walls. Finally, we show an additional plot of the components of the STT with vanishing relaxation $\beta = 0$.

Explicit expressions of the spin-transfer torque

Starting from the Ansatz

$$\mathbf{J}_r = a_r\overline{\mathbf{m}}_r + b_r\overline{\partial_{(r)}\mathbf{m}}_r + c_r\overline{\mathbf{m}}_r \times \overline{\partial_{(r)}\mathbf{m}}_r \ , \tag{9}$$

and with $\partial_{(r)}\overline{\mathbf{m}}_r = \frac{\partial_{(r)}\mathbf{n}}{|\mathbf{m}_r|} - \frac{\overline{\mathbf{m}}_r\cdot\partial_{(r)}\mathbf{n}}{|\mathbf{m}_r|}\overline{\mathbf{m}}_r$, the STT $\mathbf{T} = -\Delta_{\mathrm{sd}}\mathbf{n}\times\sum_r \mathbf{J}_r$ can be calculated. Its components in Eq. (5) are obtained as

$$\begin{aligned}
T_\nu^{\mathrm{ad}} =& \frac{\Delta_{\mathrm{sd}}}{\hbar}\sum_r c_r \frac{(\mathbf{m}_r\cdot\mathbf{n})|\partial_{(r)}\mathbf{n}|}{\mathbf{m}_r^2|\partial_{(r)}\overline{\mathbf{m}}_r|}\times\begin{cases} vr & \nu = x \\ 1 & \nu = t\end{cases}\\
T_\nu^{\mathrm{non-ad}} =& -\frac{\Delta_{\mathrm{sd}}}{\hbar}\sum_r b_r \frac{|\partial_{(r)}\mathbf{n}|}{|\mathbf{m}_r||\partial_{(r)}\overline{\mathbf{m}}_r|}\times\begin{cases} vr & \nu = x \\ 1 & \nu = t\end{cases}\\
H_{\mathrm{R}} =& \frac{\Delta_{\mathrm{sd}}\alpha_{\mathrm{R}}}{\hbar\gamma_0}\sum_r p\left(\frac{a_r}{|\mathbf{m}_r|} - b_r\frac{\mathbf{m}_r\cdot\partial_{(r)}\mathbf{n}}{\mathbf{m}_r^2|\partial_{(r)}\mathbf{m}_r|}\right).
\end{aligned} \tag{10}$$

Solution of the differential equation for wide domain walls

We show how the standard solutions for the STT are recovered in the form of [11]

$$\mathbf{T} = \tilde{T}^{\mathrm{ad}}\partial_x\mathbf{n} + \tilde{T}^{\mathrm{nonad}}\mathbf{n}\times\partial_x\mathbf{n} - H_{\mathrm{R}}\mathbf{n}\times\mathbf{e}_y \tag{11}$$

as the limiting case of an infinitely wide domain wall (DW) from the differential equation. Here, the standard expressions [11] $\tilde{T}^{\mathrm{ad}} = I_s$, $\tilde{T}^{\mathrm{nonad}} = -\beta I_s$ and $H_{\mathrm{R}} = \Delta_{\mathrm{sd}}\alpha_{\mathrm{R}}I_s/(v\hbar)$ are known. To derive this result, we use a slightly modified Ansatz

$$\mathbf{J}_r = a_r\overline{\mathbf{m}}_r + rv\tilde{b}_b\partial_x\overline{\mathbf{m}}_r + rv\tilde{c}_r\overline{\mathbf{m}}_r\times\partial_x\overline{\mathbf{m}}_r. \tag{12}$$

Here, we have not normalized the derivatives and have excluded the temporal derivatives from the beginning. With this Ansatz, a slightly modified differential equation results in the form

$$vp\partial_x\begin{pmatrix}a_r\\ \tilde{b}_r\\ \tilde{c}_r\end{pmatrix} = A_r\begin{pmatrix}a_r\\ \tilde{b}_r\\ \tilde{c}_r\end{pmatrix} + \frac{\Delta_{\mathrm{sd}}\beta}{\hbar}\begin{pmatrix}\overline{\mathbf{m}}_r\cdot\mathbf{J}_r^{\mathrm{rel}}\\ \partial_x\overline{\mathbf{m}}_r\cdot\mathbf{J}_r^{\mathrm{rel}}\\ (\overline{\mathbf{m}}_r\times\partial_x\overline{\mathbf{m}}_r)\cdot\mathbf{J}_r^{\mathrm{rel}},\end{pmatrix} \tag{13}$$

with $\mathbf{J}_r^{\mathrm{rel}} = a_r^{(0)}\mathbf{n}$ and $\sum_r va_r^{(0)} = I_s$. The coefficient matrix $A_r(x,t)$ now reads

$$A_r = \begin{pmatrix}-\Delta_{\mathrm{sd}}\beta/\hbar & v^2|\partial_x\overline{\mathbf{m}}_r|^2 & 0\\ -1 & -\Delta_{\mathrm{sd}}\beta/\hbar - f & -\Delta_{\mathrm{sd}}|\mathbf{m}_r|/\hbar - g\\ 0 & \Delta_{\mathrm{sd}}|\mathbf{m}_r|/\hbar + g & -\Delta_{\mathrm{sd}}\beta/\hbar - f\end{pmatrix} \tag{14}$$

with $f = rv(\partial_x\overline{\mathbf{m}}_r\cdot\partial_x^2\overline{\mathbf{m}}_r)/(\partial_x\overline{\mathbf{m}}_r)^2$ and $g = rv[\partial_x\overline{\mathbf{m}}_r\cdot(\overline{\mathbf{m}}_r\times\partial_x^2\overline{\mathbf{m}}_r)]/(\partial_x\overline{\mathbf{m}}_r)^2$. Since $\partial_x\mathbf{m}_r\propto\partial_x\mathbf{n}\propto 1/\lambda$, we can neglect all derivatives in Eq. (13) in the limit of a broad DW with $\lambda\to\infty$. When we further assume constant coefficients $a_r, \tilde{b}_r$ and $\tilde{c}_r$ and set $|\alpha_{\mathrm{R}}|\ll 1$, Eq. (13) reduces to a purely algebraic system of equations

$$\begin{aligned}
0 =& a_r - a_r^{(0)},\\
0 =& -a_r - \frac{\Delta_{\mathrm{sd}}\beta}{\hbar}\tilde{b}_r - \frac{\Delta_{\mathrm{sd}}}{\hbar}\tilde{c}_r,\\
0 =& \frac{\Delta_{\mathrm{sd}}}{\hbar}\tilde{b}_r - \frac{\Delta_{\mathrm{sd}}\beta}{\hbar}\tilde{c}_r.
\end{aligned} \tag{15}$$

The solutions are $a_r = a_r^{(0)}$, $\tilde{b}_r = -a_r^{(0)}\beta\hbar/[\Delta_{\mathrm{sd}}(1+\beta^2)]$ and $\tilde{c}_r = -a_r^{(0)}\hbar/[\Delta_{\mathrm{sd}}(1+\beta^2)]$. Thus, we get the STT $\mathbf{T} = -\Delta_{\mathrm{sd}}\mathbf{n}\times\sum_r\mathbf{J}_r$ in the final form of

$$\mathbf{T} \overset{|\alpha_{\mathrm{R}}^2|,\beta^2\ll 1}{=} I_s\partial_x\mathbf{n} - \beta I_s\mathbf{n}\times\partial_x\mathbf{n} - \frac{\Delta_{\mathrm{sd}}\alpha_{\mathrm{R}}I_s}{v\hbar}\mathbf{n}\times\mathbf{e}_y. \tag{16}$$

In fact, these are the standard solutions for the (non)adiabatic STT and the Rashba field-like torque.

It can be easily recognized how much the STT at small DW widths differs from the "broad DW limit" in the definition of Eq. (11) from numerical calculations. In Fig. 5 we show the STT for several DW widths – for simplicity for a vanishing α_{R}. While for $\lambda = 100\Delta_{\mathrm{osc}}$ the results of Eq. (16) are recovered, the components for smaller DW widths actually differ at and away from the DW center. This happens when the DWs are too steep to allow the spin current density to remain aligned mainly parallel to the magnetization $\mathbf{n}$, as it can be seen in Fig. (5) from the component in $\mathbf{n}$ direction. Since the electron spin can change its orientation due to the *sd* interaction over a length scale of the order $x_{\mathrm{osc}}^{\infty} = \hbar v/\Delta_{\mathrm{sd}}$ it may be almost unchanged for $\lambda \ll x_{\mathrm{osc}}^{\infty}$. As the magnetic domains change in this length scale from $\mathbf{n}(x < x_{\mathrm{DW}}) \to -\mathbf{n}(x > x_{\mathrm{DW}})$ it means an anti-parallel aligned electron spin. In fact, for a perfect anti-parallel alignment and $\beta = 0$ the electron spin $\mathbf{s}$ would never change back to a parallel alignment as it would provide no finite torque $\mathbf{T} = -\Delta_{\mathrm{sd}}\mathbf{n}\times\mathbf{s}$. With a finite β the electron spin eventually relaxes back to the parallel alignment, but for typical $\beta \ll 1$ on an even larger length scale $x_{\mathrm{damp}} = x_{\mathrm{osc}}^{\infty}/\beta$.

From the results above we find that a STT description containing a constant spin current density exceeds is reliability for steep magnetic textures.

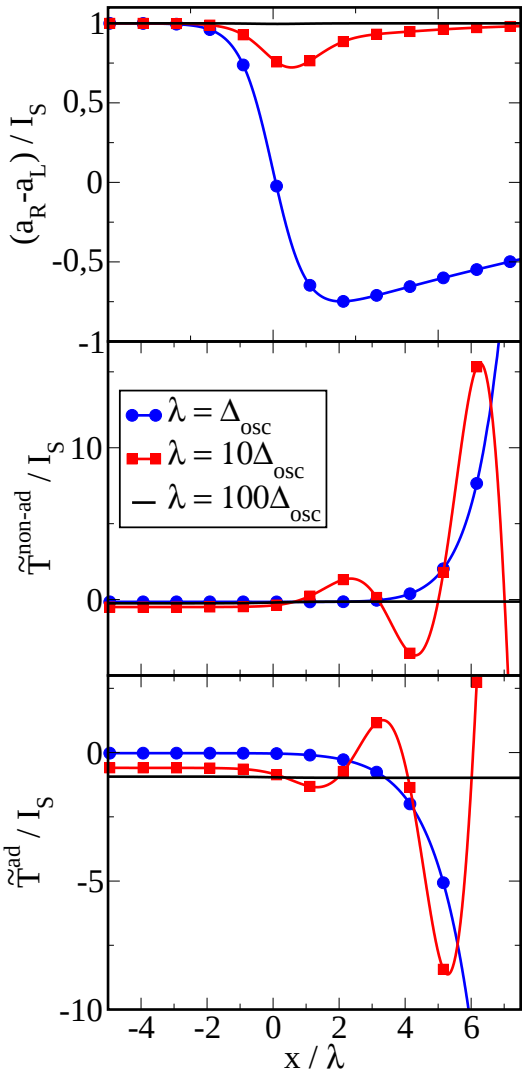

FIG. 5. (Color online) Components of the STT $\mathbf{T} = \tilde{T}^{\mathrm{non-ad}}\partial_x\mathbf{n} + \tilde{T}^{\mathrm{ad}}\mathbf{n}\times\partial_x\mathbf{n}$ vs. reduced distance from the DW center for three different DW widths. In addition, the magnitude of the spin current density in $\mathbf{n}$-direction, $a_R - a_L$, is shown. Note that the components are defined according to the non-normalized derivatives of $\mathbf{n}$. Parameters are $\alpha_{\mathrm{R}} = 0$ and $\beta = 0.2$.

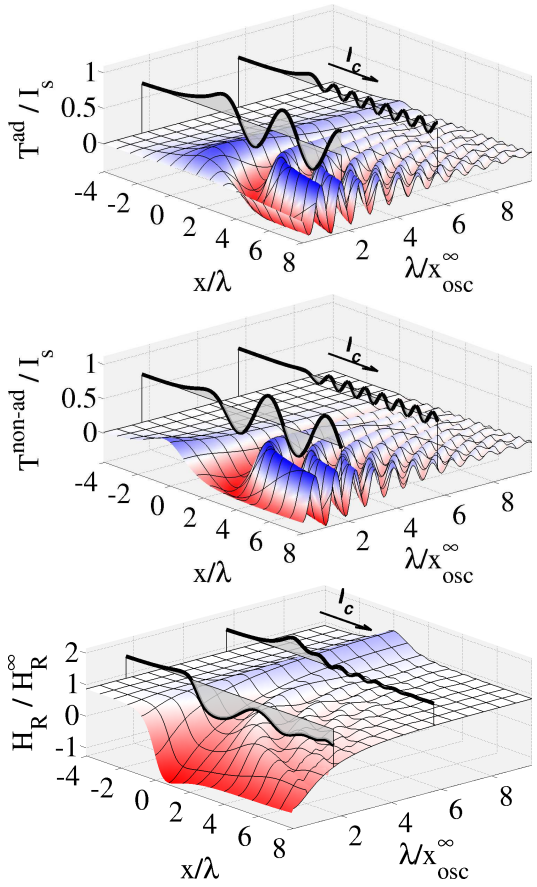

FIG. 6. (Color online) Spatial dependence of the (non)adiabatic STT and the Rashba field vs the reduced DW width $\lambda/x^{\infty}_{\mathrm{osc}}$ for $\beta = 0$. Blue (red) values indicate positive (negative) deviations from the standard solutions. In addition, the spatial dependence at two DW distinct widths $\lambda/x^{\infty}_{\mathrm{osc}} = 1.7, 5.7$ is highlighted (shifted thick black curves). No damping of the STT's oscillations occurs. We have set $\alpha_{\mathrm{R}} = 0.4$.

Components of the spin-transfer torque without relaxation

In the absence of any relaxation, i.e., $\beta = 0$, neither the adiabatic nor the nonadiabatic STT approaches the standard stationary solutions after the current has crossed the domain wall center x_{DW}. Deviations from a non-parallel alignment are not damped and may exist over a very long distance. This can be seen in Fig. 6, where we plotted the STT components according to the definition in Eq. (5) as it allows for more covenient physical interpretation. Actually, oscillations with a period of $2\pi v\hbar/\Delta_{\mathrm{sd}}$ are sustained for all $x > x_{DW}$ for both the adiabatic and the nonadiabatic torque. This, of course, also means a finite torque far away from the DW, even though, due to the oscillatory nature, the averaged force on the magnetic moments may vanish.

It is interesting to realize that even without a finite β, a strong nonadiabatic STT arises for steep magnetic textures, i.e., small λ. This is connected to the non-alignment of the itinerant electron spins and local moments at the DW and after passing the steep magnetic structure (cf. Fig. 1).

[1] G. Beach, M. Tsoi, and J. Erskine, J. Magn. Magn. Mater. **320**, 1272 (2008).
[2] K. Obata and G. Tatara, Phys. Rev. B **77**, 214429 (2008).
[3] S. S. Parkin, M. Hayashi, and L. Thomas, Science **320**, 190 (2008).

[4] X. Yu, N. Kanazawa, W. Zhang, T. Nagai, T. Hara, K. Kimoto, Y. Matsui, Y. Onose, and Y. Tokura, Nature communications **3**, 988 (2012).

[5] N. Romming, C. Hanneken, M. Menzel, J. E. Bickel, B. Wolter, K. von Bergmann, A. Kubetzka, and R. Wiesendanger, Science **341**, 636 (2013).

[6] M. E. Knoester, J. Sinova, and R. A. Duine, Phys. Rev. B **89**, 064425 (2014).

[7] A. A. Khajetoorians, J. Wiebe, B. Chilian, and R. Wiesendanger, Science **332**, 1062 (2011).

[8] J. Zang, M. Mostovoy, J. H. Han, and N. Nagaosa, Phys. Rev. Lett. **107**, 136804 (2011).

[9] M. Bode, M. Heide, K. Von Bergmann, P. Ferriani, S. Heinze, G. Bihlmayer, A. Kubetzka, O. Pietzsch, S. Blügel, and eq::dgl R. Wiesendanger, Nature **447**, 190 (2007).

[10] A. Thiaville, S. Rohart, É. Jué, V. Cros, and A. Fert, Europhys. Lett. **100**, 57002 (2012).

[11] Z. Li and S. Zhang, Phys. Rev. B **70**, 024417 (2004).

[12] L. Heyne, J. Rhensius, D. Ilgaz, A. Bisig, U. Rüdiger, M. Kläui, L. Joly, F. Nolting, L. J. Heyderman, J. U. Thiele, and F. Kronast, Phys. Rev. Lett. **105**, 187203 (2010).

[13] S. Rößler, S. Hankemeier, B. Krüger, F. Balhorn, R. Frömter, and H. P. Oepen, Phys. Rev. B **89**, 174426 (2014).

[14] K. Sekiguchi, K. Yamada, S.-M. Seo, K.-J. Lee, D. Chiba, K. Kobayashi, and T. Ono, Phys. Rev. Lett. **108**, 017203 (2012).

[15] D. Claudio-Gonzalez, A. Thiaville, and J. Miltat, Phys. Rev. Lett. **108**, 227208 (2012).

[16] X. Waintal and M. Viret, EPL (Europhysics Letters) **65**, 427 (2004).

[17] J. Xiao, A. Zangwill, and M. D. Stiles, Phys. Rev. B **73**, 054428 (2006).

[18] S. Bohlens and D. Pfannkuche, Phys. Rev. Lett. **105**, 177201 (2010).

[19] T. Taniguchi, J. Sato, and H. Imamura, journal Phys. Rev. B **79**, 212410 (2009).

[20] G. Tatara, H. Kohno, J. Shibata, Y. Lemaho, and K.-J. Lee, Journal of the Physical Society of Japan **76**, 054707 (2007).

[21] A. K. Nguyen, H. J. Skadsem, and A. Brataas, Phys. Rev. Lett. **98**, 146602 (2007).

[22] X. Wang and A. Manchon, Phys. Rev. Lett. **108**, 117201 (2012).

[23] J.-i. Ohe and B. Kramer, Phys. Rev. Lett. **96**, 027204 (2006).

[24] C. A. Akosa, W.-S. Kim, A. Bisig, M. Kläui, K.-J. Lee, and A. Manchon, Phys. Rev. B **91**, 094411 (2015).

[25] A. Brataas and K. M. Hals, Nature nanotechnology **9**, 86 (2014).

[26] K. M. D. Hals and A. Brataas, Phys. Rev. B **89**, 064426 (2014).

[27] M. Thorwart and R. Egger, Phys. Rev. B **76**, 214418 (2007).

[28] M. Stier, R. Egger, and M. Thorwart, Phys. Rev. B **87**, 184415 (2013).

[29] M. Stier, M. Creutzburg, and M. Thorwart, Phys. Rev. B **90**, 014433 (2014).

[30] A. O. Gogolin, A. A. Nersesyan, and A. M. Tsvelik, *Bosonization and strongly correlated systems* (Cambridge University Press, 2004).

[31] X. Zhou, Z. Zhang, and C.-Z. Hu, arXiv:0904.3796.

[32] Q.-f. Sun and X. C. Xie, Phys. Rev. B **72**, 245305 (2005).

[33] S. Zhang and Z. Li, Phys. Rev. Lett. **93**, 127204 (2004).

[34] J. Shi, P. Zhang, D. Xiao, and Q. Niu, Phys. Rev. Lett. **96**, 076604 (2006).

[35] M. E. Lucassen, H. J. van Driel, C. M. Smith, and R. A. Duine, Phys. Rev. B **79**, 224411 (2009).

[36] J. Linder and M. Alidoust, Phys. Rev. B **88**, 064420 (2013).

[37] L. Thomas and S. Parkin, "Current induced domain-wall motion in magnetic nanowires," in *Handbook of Magnetism and Advanced Magnetic Materials* (John Wiley & Sons, Ltd, 2007).